

A Comparison of the Noise Sensitivity of Nine *QRS* Detection Algorithms

GARY M. FRIESEN, THOMAS C. JANNETT, MEMBER, IEEE, MANAL AFIFY JADALLAH,
STANFORD L. YATES, STEPHEN R. QUINT, MEMBER, IEEE,
AND H. TROY NAGLE, FELLOW, IEEE

Abstract—The noise sensitivities for nine different *QRS* detection algorithms were measured for a normal, single-channel lead II, synthesized ECG corrupted with five different types of synthesized noise. The noise types were electromyographic interference, 60 Hz powerline interference, baseline drift due to respiration, abrupt baseline shift, and a composite noise constructed from all of the other noise types. The percentage of *QRS* complexes detected, the number of false positives, and the detection delay were measured.

None of the algorithms were able to detect all *QRS* complexes without any false positives for all of the noise types at the highest noise level. Algorithms based on amplitude and slope had the highest performance for EMG-corrupted ECG. An algorithm using a digital filter had the best performance for the composite noise corrupted data.

I. INTRODUCTION

IN recent years the trend toward automated analysis of electrocardiograms has gained momentum. Many systems have been implemented in order to perform such tasks as 12-lead off-line electrocardiogram analysis, Holter tape analysis, and real-time patient monitoring. Recent literature dealing with design consideration of cardiac pacemakers suggests that the latest generation of these devices employs an ECG analysis capability. All of these applications require the accurate detection of *QRS* complexes in the presence of noise. Many of the existing ECG analysis programs require a relatively noise-free digitized ECG. Data corrupted with noise must either be filtered or discarded. ECG quality assurance not only requires human or software noise detection schemes, but can also result in the loss of clinically significant data. Filtering can alter the signal and may require substantial computational overhead. These issues are important design consideration for applications in real-time heart monitoring.

Manuscript received November 16, 1987; revised September 2, 1988. This work was supported by the Engineering Experiment Station at Auburn University and the North Carolina Biotechnology Center.

G. M. Friesen is with Auburn University, Auburn, AL 36830.

T. C. Jannett is with the Department of Electrical Engineering, University of Alabama, Birmingham, AL, 35233.

M. A. Jadallah is with Alcatel Network Systems, Research Triangle Park, NC.

S. L. Yates is with Bell Northern Research, Research Triangle Park, NC.

S. R. Quint is with the Biomedical Engineering Curriculum, University of North Carolina, Chapel Hill, NC 27514.

H. T. Nagle is with the Department of Electrical and Computer Engineering North Carolina State University, Raleigh, NC 27695.

IEEE Log Number 8931541.

The purpose of this paper is to quantify the relative noise susceptibility of nine different *QRS* detection schemes. The database consists of a *synthesized* normal ECG (used as a *gold standard*) corrupted with four levels of each of four types of noise. These four noise types were also combined to form a fifth composite noise source. The ability of each algorithm to detect *QRS* complexes and to locate the onset of each complex was measured on each noise-corrupted ECG as well as on the noise-free ECG. The nine *QRS* detection algorithms were chosen from a literature survey. Each algorithm was programmed in Fortran from its published description. The algorithms are nonadaptive. In programming each one, we attempted to implement the essential features described by its authors. When possible, we tuned each algorithm for the noise sources we are applying by adjusting its parameters (thresholds, weighting constants, etc.). In other words, we attempted to make each of the nine *QRS* algorithms perform at its best for our five noise types. The input signal to all nine algorithms is a synthesized, ideal, invariant ECG. Consequently, the exact location of the *QRS* complex is known before the noise sources are added.

The results of this study will help in the development of a more robust clinical instrument by making the front-end signal processing more effective. A procedure to be followed might be:

- 1) Evaluate a *QRS* detection algorithm by using a *gold standard* ECG waveform;
- 2) evaluate a *QRS* detection algorithm using a set standard ECG waveforms such as the MIT/BIH database;
- 3) implement the algorithm in a VLSI chip with built-in self test features; and
- 4) include the chip in a prototype clinical instrument.

This paper addresses the techniques in step 1).

In the next section we discuss the properties of noise artifacts in ECG signals. Then we select certain features of the artifacts for our noise simulation. Next we describe the details of our implementation of the nine *QRS* algorithms. Finally we present the simulation results and compare the algorithms' performance.

II. NOISE ARTIFACTS IN ECG'S

Electrocardiographic (ECG) signals may be corrupted by various kinds of noise. Typical examples are:

- 1) power line interference
- 2) electrode contact noise
- 3) motion artifacts
- 4) muscle contraction (electromyographic, EMG)
- 5) baseline drift and ECG amplitude modulation with respiration

6) instrumentation noise generated by electronic devices used in signal processing, and

- 7) electrosurgical noise,

and other, less significant noise sources [1]. A brief description of each noise signal listed will be given below, and methods for approximating these signals will be discussed. Identification of the pertinent characteristics of each noise signal will be given.

A. Power Line Interference

Power line interference consists of 60 Hz pickup (in the U.S.) and harmonics which can be modeled as sinusoids and combination of sinusoids [2]. See Fig. 1(a). Characteristics which might need to be varied in a model of power line noise include the amplitude and frequency content of the signal. These characteristics are generally consistent for a given measurement situation and, once set, will not change during a detector evaluation.

Typical parameters:

Frequency content—60 Hz (fundamental) with harmonics

Amplitude—up to 50 percent of peak-to-peak ECG amplitude

B. Electrode Contact Noise

Electrode contact noise is transient interference caused by loss of contact between the electrode and skin, which effectively disconnects the measurement system from the subject. See Fig. 1(b). The loss of contact can be permanent, or can be intermittent, as would be the case when a loose electrode is brought in and out of contact with the skin as a result of movements and vibration. This switching action at the measurement system input can result in large artifacts since the ECG signal is usually capacitively coupled to the system. With the amplifier input disconnected, 60 Hz interference may be significant.

Electrode contact noise can be modeled as a randomly-occurring rapid baseline transition (step) which decays exponentially to the baseline value and has a superimposed 60 Hz component. This transition may occur only once or may rapidly occur several times in succession. Characteristics of this noise signal include the amplitude of the initial transition, the amplitude of the 60 Hz component, and the time constant of the decay.

Typical parameters:

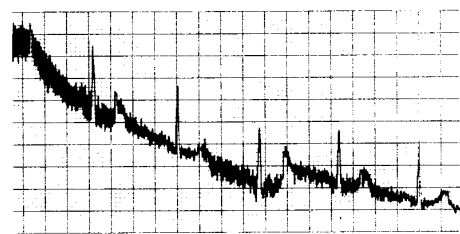
Duration—1 s

Amplitude—maximum recorder output

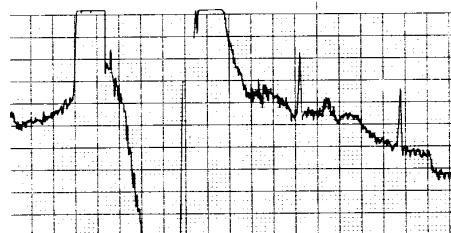
Frequency—60 Hz Time constant—about 1 s

C. Motion Artifacts

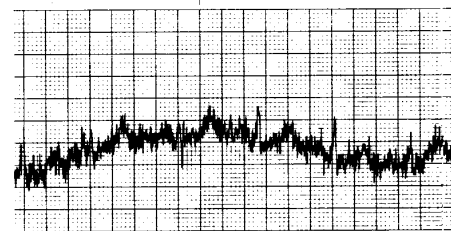
Motion artifacts are transient (but not step) baseline changes caused by changes in the electrode-skin imped-



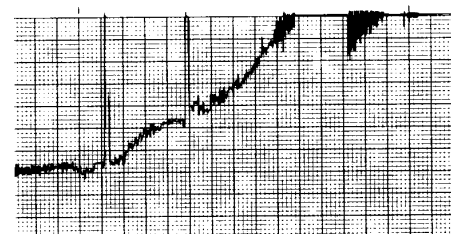
(a)



(b)



(c)



(d)

Fig. 1. Noisy electrocardiograms: (a) powerline and motion artifact; (b) loose contacts; (c) respiration and EMG; (d) Instrumentation saturation.

ance with electrode motion. A typical example is shown in Fig. 1(a). As this impedance changes, the ECG amplifier sees a different source impedance, which forms a voltage divider with the amplifier input impedance. Therefore, the amplifier input voltage depends on the source impedance, which changes as the electrode position changes. The usual cause of motion artifacts will be assumed to be vibrations or movement of the subject. The shape of the baseline disturbance caused by motion artifacts can be assumed to be a biphasic signal resembling one cycle of a sine wave. The peak amplitude and duration of the artifact are variables.

Typical parameters:

Duration—100–500 ms

Amplitude—500 percent of peak-to-peak ECG amplitude

D. Muscle Contractions (EMG)

Muscle contractions cause artifactual millivolt-level potentials to be generated. The baseline electromyogram is usually in the microvolt range and therefore is usually insignificant. As shown in Fig. 1(c), the signals resulting from muscle contraction can be assumed to be transient bursts of zero-mean band-limited Gaussian noise. The variance of the distribution may be estimated from the variance and duration of the bursts.

Typical parameters:

Standard Deviation—10 percent of peak-to-peak ECG amplitude

Duration—50 ms

Frequency Content—dc to 10 000 Hz [1]

E. Baseline Drift and ECG Amplitude Modulation with Respiration

The drift of the baseline with respiration can be represented as a sinusoidal component at the frequency of respiration added to the ECG signal. See Fig. 1(c). The amplitude and frequency of the sinusoidal component should be variables. The amplitude of the ECG signal also varies by about 15 percent with respiration. The variation could be reproduced by amplitude modulation of the ECG by the sinusoidal component which is added to the baseline.

Typical parameters:

Amplitude variation—15 percent of peak-to-peak (p-p) ECG amplitude

Baseline variation—15 percent of p-p ECG amplitude variation at 0.15 to 0.3 Hz

F. Noise Generated by Electronic Devices Used in Signal Processing

Artifacts generated by electronic devices in the instrumentation system as shown in Fig. 1(d) cannot be corrected by a *QRS* detection algorithm. The input amplifier has saturated and no information about the ECG can reach the detector. In this case an alarm must sound to alert the ECG technician to take corrective action.

G. Electrosurgical Noise

Electrosurgical noise completely destroys the ECG and can be represented by a large amplitude sinusoid with frequencies approximately between 100 kHz and 1 MHz. Since the sampling rate of an ECG signal is 250 to 1000 Hz, an aliased version of this signal would be added to the ECG signal. The amplitude, duration, and possibly the aliased frequency should be variable.

Typical parameters:

Amplitude—200 percent of peak-to-peak ECG amplitude

Frequency Content—Aliased 100 kHz to 1 MHz Duration—1–10 s

III. THE ECG DATABASE

A. The Uncorrupted Signal

The uncorrupted signal was obtained by recording the Lead II ECG of a human volunteer on a Beckman analog ECG strip chart recorder inside a shielded instrumentation cage. This recording was manually digitized. The digitized single cycle of the ECG was copied and appended to itself repetitively in order to form 37 cycles of the ECG for a total of 32 s of data. The digitized ECG was plotted on a graphics terminal and subsequently edited until it appeared consistent with the analog recording. The digitized ECG was then transferred to a VAX 11/780. The digitized ECG has an equivalent sampling rate of 250 Hz, and is stored in a Fortran data file as a linear array of 8192 single precision floating point numbers. The heart rate is a constant 69 beats per min, the *QRS* width is 88 ms, and the *R*-wave amplitude is 1.08 mV. These characteristics fall within the normal range according to Ganong [3]. A plot of a segment of the normal, uncorrupted ECG appears in Fig. 2.

B. The Simulated Noise

Since the purpose of this study was to evaluate the noise rejection properties of nine *QRS* detection algorithms, we selected four different representative noise sources for simulation:

- 1) electromyographic interference because of its random properties and high frequency content,
- 2) powerline interference because it is ubiquitous,
- 3) baseline drift due to respiration because of its low frequency properties,
- 4) abrupt shifts in the baseline due to its large first derivative, and
- 5) a composite of all of the above.

Although we did not specifically simulate electrosurgical and instrumentation noise, they behave similarly to the random model we use for EMG. Using the same reasoning, motion artifact is much like baseline drift in respiration so it also was not specifically modeled.

Now let us describe our noise models more precisely. In what follows, the dynamic characteristics of the five noise types are specified. In each case, the maximum amplitude was selected well beyond the values of the typical parameters given earlier to challenge the algorithms while allowing reasonable results at intermediate noise levels. Each of the five types of noise is added to an uncorrupted ECG at four different levels: 25, 50, 75, and 100 percent of the maximum amplitude.

1) *Electromyographic Interference*: This type of noise is simulated by adding random noise to the ECG. The maximum noise level is formed by adding random single precision numbers of ± 50 percent of the ECG maximum amplitude to the uncorrupted ECG. The reduced noise levels are formed by scaling the random numbers by the appropriate amount. The random numbers are generated using the VAX-11 Fortran random number generator. A

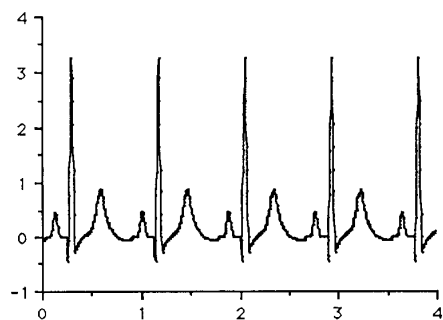


Fig. 2. Uncorrupted ECG.

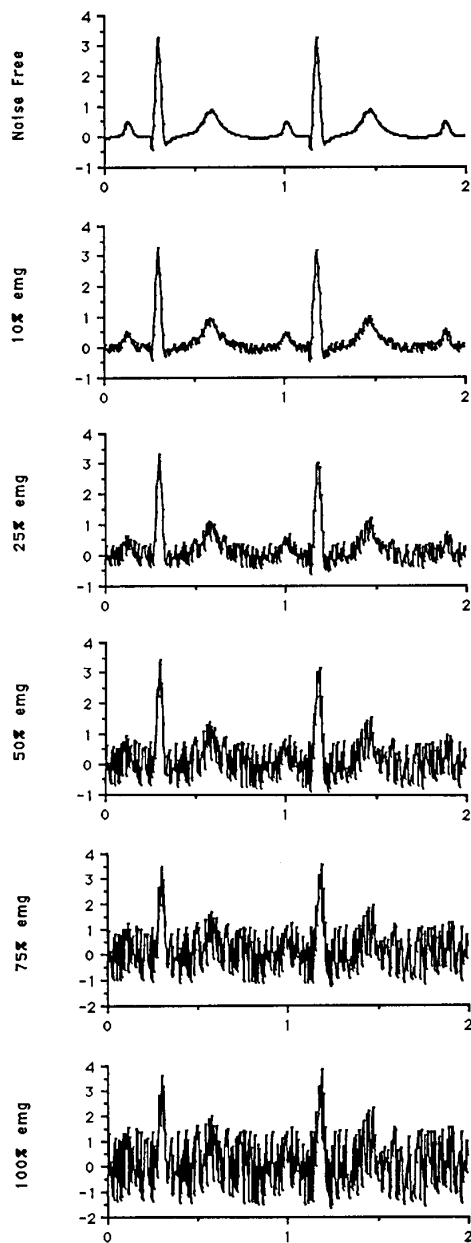


Fig. 3. ECG corrupted with electromyographic noise.

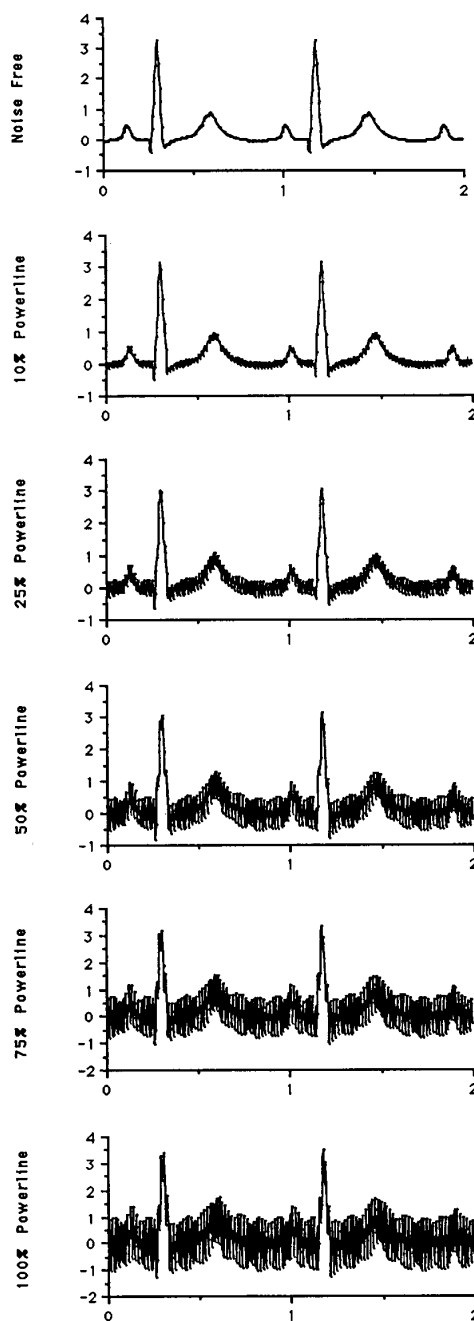


Fig. 4. ECG corrupted with 60 Hz powerline interference.

plot of the ECG corrupted by electromyographic noise is given in Fig. 3.

2) *Powerline Interference*: Sixty Hertz noise is generated using the Fortran sine function generator. The maximum noise level corresponds to a peak-to-peak amplitude of 0.333 mV. A plot of the ECG corrupted by this type of noise is given in Fig. 4. Harmonic powerline line frequencies were not modeled since the 60 Hz component will be dominant.

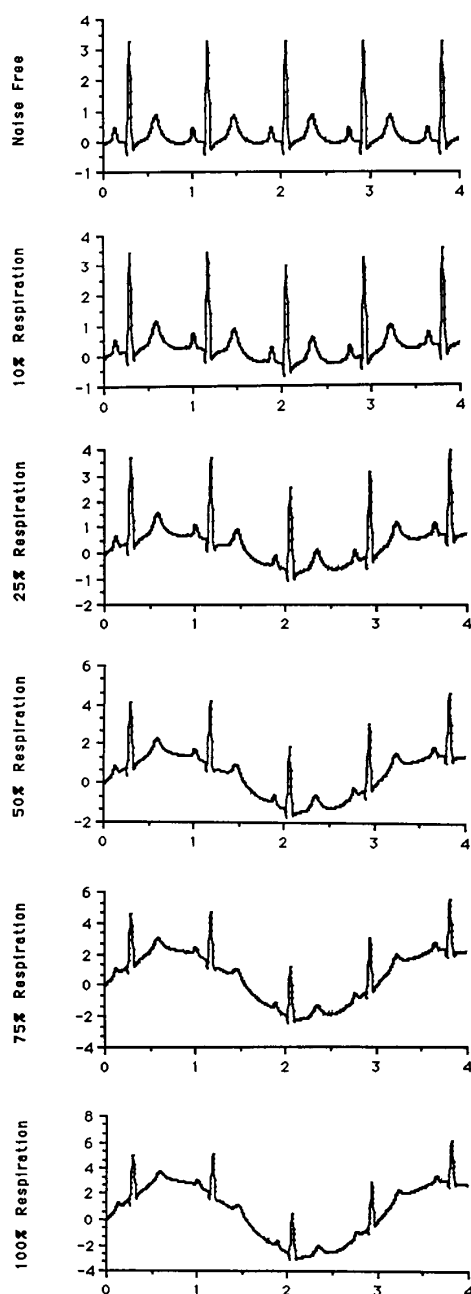


Fig. 5. ECG corrupted with baseline drift due to respiration.

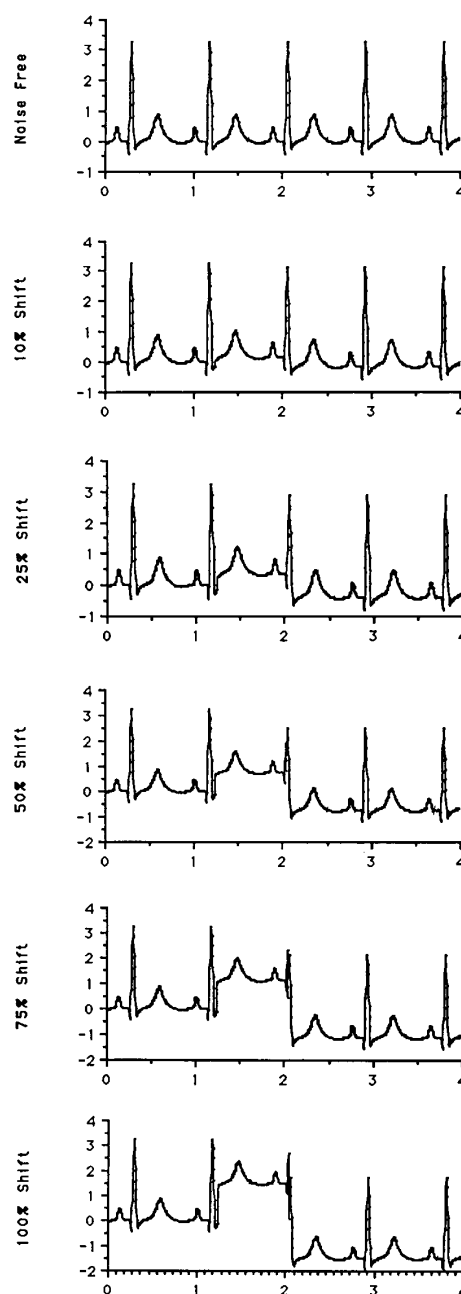


Fig. 6. ECG corrupted with abrupt baseline shift.

3) *Baseline Drift Due to Respiration*: This type of interference is simulated by adding a low frequency sinusoid to the uncorrupted ECG. The frequency is 0.333 Hz and the maximum amplitude is 1.0 mV peak. It is generated in the same manner as the powerline interference, except that the frequency and the maximum amplitude are different. Amplitude effects due to respiration were not modeled. A plot of the ECG corrupted by baseline drift due to respiration is given in Fig. 5.

4) *Abrupt Shift in Baseline*: This type of interference represents an abrupt shift in baseline due to movement of the patient while the ECG is being recorded. It is simulated by adding a dc bias for a given segment of the ECG. The maximum noise level consists of six alternating baseline shifts of +0.5 or -0.5 mV. This resulted in five baseline shifts of +1.0 or -1.0 mV and one of +0.5 mV. The reduced noise levels are scaled by the appropriate amount. A plot of the ECG corrupted by abrupt shifts in

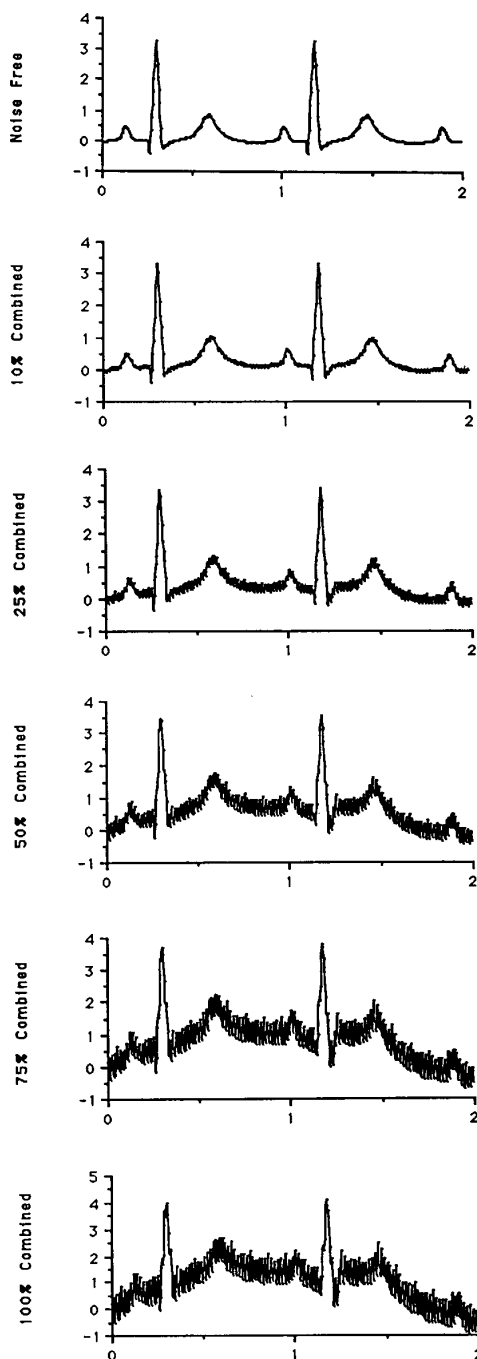


Fig. 7. ECG corrupted with composite noise.

baseline appears in Fig. 6. In reality, shifts in ECG baselines are less abrupt than our model; hence we are performing a worst case simulation for the derivative-based *QRS* algorithms.

5) *Composite Noise*: A composite noise is constructed by combining all of the noise types described above. The maximum noise level is constructed by reducing the maximum noise levels for each of the previously described

noise types to 50 percent of maximum and then summing them. The reduced noise levels of the composite are formed by scaling the composite noise after it has been formed and then adding it to the uncorrupted ECG. A plot of the ECG's corrupted by the composite is given in Fig. 7.

IV. METHODS

A. The Software Structure

The software for this experiment is written in VAX-11 Fortran and executed on a VAX-11/780 computer. The software package consists of five major components. The collection of algorithms and digitized ECG data files make up two of the components. A scoring routine and a routine to tabulate the results account for two additional blocks. The fifth module is a main program which integrates the four modules listed above. The algorithms are called sequentially. Each of the data files illustrated in Figs. 2–7 are submitted to the algorithm for *QRS* detection. When an algorithm detects a *QRS* candidate, the scoring routine is called by the algorithm. Following the scoring procedure, the algorithm resumes its search for the next *QRS* starting at the next data point until the next *QRS* candidate is detected or until the data is exhausted. This procedure continues until all of the algorithms have been run on each of the ECG data files. The results are then tabulated.

B. The Scoring Criteria

The scoring routine compares the onset of the *QRS* candidate to a key file containing the locations of all of the valid *QRS* onsets. If the candidate onset falls between the actual onset and the end of the *QRS* complex (22 sample points or 88 ms following the actual onset), it is scored as a *QRS* detection. If the candidate onset occurs outside of these boundaries, it is counted as a false positive. The percentage of *QRS* complexes correctly detected is calculated at the end of each run by dividing the number of *QRS* complexes correctly detected by the total number of actual *QRS* complexes.

An indication of the average time delay required for detection is also calculated after each run. If the detection occurs after the actual onset but before the end of the *QRS* complex, it is classified as a late detection. The number of sample points between the onset and the detection are summed for all of the detections of that run. This number is divided by the total number of detections to give the average time delay (in 4 ms sample points).

Since the search for the next *QRS* complex resumes at the next sample point following the candidate onset, it is possible that the same *QRS* complex will be detected more than once. Only the first correct detection will be included in the scoring of *QRS*-complexes found or the measure of delay. Subsequent detections which fall within the boundaries of the first detected *QRS* should be ignored.

In some systems, the search for the next *QRS* does not resume until a minimum delay has passed. This delay, or window, corresponds to the minimum distance to the next *QRS* complex based on the maximum possible heart rate.

This method was not used since false positives could be skipped over, or a valid *QRS* complex might be overlooked if the *QRS* candidate was actually a false positive located just before the real *QRS* complex. In our study, we did not use the windowing approach *per se* since it would enhance the performance of the nine algorithms. We did adjust our scoring algorithm so that multiple detections of the same *QRS* would not result in a penalty.

V. DESCRIPTION OF THE ALGORITHMS

A. Algorithm Selection Criteria

A large number of *QRS* detection schemes are described in the literature [2], [4]–[37]. It would be impractical to compare all of them. Several considerations were used to limit the number of *QRS* detections schemes to a reasonable cross section of the different basic techniques described in the literature.

The two basic criteria used in selection were complexity and performance. Only relatively simple algorithms were used. Any of the algorithms used in this study could easily execute in real-time on a common 8-bit microprocessor with enough reserve processing capacity for other related functions such as preprocessing or ECG analysis capabilities. Certain schemes, such as Holter tape analysis, require faster than real-time capability which places even more importance on this restriction.

The performance criterion was the basis for rejecting *QRS* detection algorithms which were highly noise sensitive and gave large numbers of false positives at low noise levels. All of the algorithms should be insensitive to low noise levels if they are to be realistic candidates for incorporation in clinical systems.

Each algorithm in this study is based on a specific scheme presented in the literature. However, they are not copies and should be considered as a generic adaptation of the fundamental concept. A great deal of experimentation was used to determine which of the available *QRS* detection algorithms were to be used and to determine the exact form of the adaptation. There are four basic types of algorithms included in this study with at least two variants of each type. The basic type is designated by a two letter prefix “AF” for algorithms based on both amplitude and first derivative, “FD” for algorithms based on first derivative only, “FS” algorithms utilize both first and second derivative, and the last category was designated “DF” which refers to digital *QRS* pass filters.

B. Algorithm Parameter Determination

Each of the algorithms used in this study employed one or more preset constants, either as multipliers or as thresholds. In some cases these constants were not given in the literature, while in others they were not compatible with the data format that we used. A tuning procedure was carried out in order to determine the value for these constants which would give the best results for the composite noise corrupted data. The approximate values of these constants were determined by observing intermediate

stages of the algorithms when the normal uncorrupted ECG was applied. The precise value of these constants was determined by varying each of the constants in an algorithm independently and recording the combinations of constants which gave the best results when the 75 or 100 percent composite noise corrupted ECG was applied, preference given to the highest noise level that allowed reasonable results. The rough constants were varied from approximately 75 to 125 percent of the preliminary value using at least ten different increments. If any of the final values of the constants fell on or near the end points, the process was repeated using the final value from the previous run as the starting point for the next run. The scoring criteria for the selection of the constants were based on obtaining the highest possible value for the difference between the number of *QRS* complexes correctly detected and the number of false positives. If a range of values of a particular constant gave equally good results, the process was carried out on the 75 and 100 percent levels of the other types of noise. The results of these runs suggested the values of the constants. Finally, the algorithm was executed on all of the noise-corrupted data and the results were tabulated. The results were checked to insure that no decrease in performance had occurred following the final selection of the constants compared to the best results obtained during the tuning procedure.

C. Algorithms Based on Amplitude and First Derivative

1) *AF1*: The concept for this *QRS* complex detector was derived from the algorithm developed by Moriet-Mahoudeaux [4]. Let $X(n) = X(0), X(1), \dots, X(8191)$ represent a one-dimensional array of sample points of the synthesized digitized ECG. An amplitude threshold is calculated as a fraction of the largest positive valued element of that array

$$\begin{aligned} \text{Amplitude threshold} \\ = 0.3 \max [X(n)] \quad 0 < n < 8191. \end{aligned}$$

The first derivative $Y(n)$ is calculated at each point of $X(n)$ such that

$$Y(n) = X(n+1) - X(n-1) \quad 1 < n < 8190.$$

A *QRS* candidate occurs when three consecutive points in the first derivative array exceed a positive slope threshold and are followed within the next 100 ms by two consecutive points which exceed the negative (descending slope) threshold. All data points in the ECG between the onset of the rising slope and before the end of the descending slope must meet or exceed the amplitude threshold.

$$Y(i), Y(i+1), Y(i+2) > 0.5$$

and

$$Y(j), Y(j+1) < -0.3$$

where

$$(i+2) < j < (i+25)$$

and

$$\begin{aligned} X(i), X(i+1), \dots, X(j+1) \\ \geq \text{amplitude threshold.} \end{aligned}$$

2) *AF2*: This algorithm is an adaptation of the analog *QRS* detection scheme developed by Fraden and Neuman [5]. A threshold is calculated as a fraction of the peak value of the ECG.

$$\begin{aligned} \text{Amplitude threshold} \\ = 0.4 \max [X(n)] \quad 0 < n < 8191. \end{aligned}$$

The raw data is then rectified:

$$\begin{aligned} Y0(n) &= X(n) \text{ if } X(n) \geq 0 \quad 0 < n < 8191 \\ Y0(n) &= -X(n) \text{ if } X(n) < 0 \quad 0 < n < 8191 \end{aligned}$$

The rectified ECG is passed through a low level clipper:

$$\begin{aligned} Y1(n) &= Y0(n) \text{ if } Y0(n) \geq \text{amplitude threshold} \\ Y1(n) &= \text{amplitude threshold if } Y0(n) \\ &< \text{amplitude threshold.} \end{aligned}$$

The first derivative is calculated at each point of the clipped, rectified array:

$$Y2(n) = Y1(n+1) - Y1(n-1) \quad 1 < n < 8190$$

A *QRS* candidate occurs when a point in $Y2(n)$ exceeds the fixed constant threshold,

$$Y2(i) > 0.7.$$

3) *AF3*: The concept for this algorithm was taken from Gustafson [6]. The first derivative is calculated at each point of the ECG:

$$Y(n) = X(n+1) - X(n-1) \quad 1 < n < 8190.$$

The first derivative array is then searched for points which exceed a constant threshold:

$$Y(i) \geq 0.15.$$

Then the next three derivative values $Y(i+1)$, $Y(i+2)$, and $Y(i+3)$ must also exceed 0.15.

If the above conditions are met, point i can be classified as a *QRS* candidate if the next two sample points have positive slope amplitude products:

$$Y(i+1)X(i+1) \text{ and } Y(i+2)X(i+2) > 0.$$

D. Algorithms Based on First Derivative Only

1) *FD1*: This algorithm was adapted from one developed by Menard [7]. The first derivative is calculated for each point of the ECG, using the formula specified by Menard:

$$\begin{aligned} Y(n) &= -2X(n-2) - X(n-1) + X(n+1) \\ &+ 2X(n+2) \quad 2 < n < 8189. \end{aligned}$$

The slope threshold is calculated as a fraction of the maximum slope for the first derivative array. In the original

form only the first 1.2 s of data is considered, but in this experiment the entire 32 s of ECG is used.

$$\text{Slope threshold} = 0.70 \max [Y(n)] \quad 2 < n < 8189.$$

The first derivative array was searched for points which exceed the slope threshold. The first point that exceeds the slope threshold is taken as the onset of a *QRS* candidate:

$$Y(i) > \text{slope threshold.}$$

2) *FD2*: This algorithm is a modification of an early digital *QRS* detection scheme developed by Holsinger [8]. In the original form it had an unacceptably high incidence of false positives, therefore it was substantially modified. The first derivative is calculated for the ECG.

$$Y(n) = X(n+1) - X(n-1) \quad 1 < n < 8190.$$

This array is searched until a point is found that exceeds the slope threshold:

$$Y(i) > 0.45$$

A *QRS* candidate occurs if another point in the next three sample points also exceeds the threshold:

$$Y(i+1) > 0.45, \text{ or}$$

$$Y(i+2) > 0.45, \text{ or}$$

$$Y(i+3) > 0.45.$$

This technique of requiring multiple, possibly nonadjacent sample points to define a *QRS* candidate generally allows the use of higher thresholds since noise often reduces the value of the first derivative for one or more of the sample points of the *R*-wave. The width of the region and the number of points which must exceed the threshold are determined by the tuning procedure as specified earlier.

E. Algorithms Based on First and Second Derivative

1) *FS1*: This algorithm is a simplification of the *QRS* detection scheme presented by Balda [9]. The absolute values of the first and second derivative are calculated from the ECG:

$$\begin{aligned} Y0(n) &= \text{ABS}[X(n+1) - X(n-1)] \\ 2 < n < 8189 \end{aligned}$$

$$\begin{aligned} Y1(n) &= \text{ABS}[X(n+2) - 2X(n) + X(n-2)] \\ 2 < n < 8189. \end{aligned}$$

These two arrays are scaled and then summed:

$$Y2(n) = 1.3 Y0(n) + 1.1 Y1(n) \quad 2 < n < 8189.$$

This array is scanned until a threshold is met or exceeded:

$$Y2(i) \geq 1.0.$$

Once this occurs, the next eight points are compared to the threshold. If six or more of these eight points meet or

exceed the threshold, the criteria for identification of a *QRS* candidate is met.

2) *FS2*: This algorithm was adapted from the *QRS* detection scheme developed by Ahlstrom and Tompkins [10]. The rectified first derivative is calculated from the ECG:

$$Y0(n) = \text{ABS}[X(n+1) - X(n-1)]$$

$$3 < n < 8188.$$

The rectified first derivative is then smoothed:

$$Y1(n) = [Y0(n-1) + 2Y0(n) + Y0(n+1)]/4$$

$$3 < n < 8188.$$

The rectified second derivative is calculated:

$$Y2(n) = \text{ABS}[X(n+2) - 2X(n) + X(n-2)]$$

$$3 < n < 8188.$$

The rectified, smoothed first derivative is added to the rectified second derivative:

$$Y3(n) = Y1(n) + Y2(n)$$

$$3 < n < 8188.$$

The maximum value of this array is determined and scaled to serve as primary and secondary thresholds:

$$\text{Primary threshold} = 0.8 \max[Y3(n)]$$

$$3 < n < 8188$$

$$\text{Secondary threshold} = 0.1 \max[Y3(n)]$$

$$3 < n < 8188.$$

The array of the summed first and second derivatives is scanned until a point exceeds the primary threshold. In order to be classified as a *QRS* candidate, the next six consecutive points must all meet or exceed the secondary threshold:

$$Y3(i) \geq \text{primary threshold, and}$$

$$Y3(i+1), Y3(i+2), \dots, Y3(i+6)$$

$$> \text{secondary threshold.}$$

In the original version of this algorithm, the second derivative of the rectified ECG was smoothed, presumably in the same manner as the first derivative. The performance of the original algorithm was erratic in the presence of noise and was substandard when compared to the current form as specified above.

F. Algorithms Based on Digital Filters

1) *DF1*: This algorithm is an adaptation of the one developed by Engelse and Zeelenberg [11]. The ECG is passed through a differentiator with a 62.5 Hz notch filter.

$$Y0(n) = X(n) - X(n-4) \quad 4 < n < 8191.$$

The differentiated, filtered data is then passed through a digital low-pass filter.

$$Y1(n) = Y0(n) + 4Y0(n-1) + 6Y0(n-2)$$

$$+ 4Y0(n-3) + Y0(n-4).$$

Two thresholds are used, equal in magnitude but opposite in polarity. The output of the low-pass filter is scanned until a point with amplitude greater than the positive threshold is reached. This point is the onset of a 160 ms search region. The number of alternate threshold crossings is used to classify the initial crossing as either a baseline shift, a *QRS* candidate, or as noise:

If $Y1(i) > 21.0$, then search region onset = i .

If no other threshold crossings occur within the 160 ms search region, the occurrence is classified as a baseline shift. Otherwise, the following three conditions are tested:

Condition 1: If $Y1(i+j) < -21.0$ $0 < j < 40$

Condition 2: If $Y1(i+j) < -21.0$ $0 < j < 40$,

and

$$Y1(1+k) > 21.0 \quad j < k < 40$$

Condition 3: If $Y1(i+j) < -21.0$ $0 < j < 40$,

and

$$Y1(i+k) > 21.0 \quad j < k < 40$$

and

$$Y1(i+1) < -21.0 \quad k < 1 < 40.$$

If any of the above conditions apply, the occurrence is classified as a *QRS* candidate. If additional threshold crossings occur, the occurrence is classified as noise.

2) *DF2*: This algorithm is an adaptation of Okada's *QRS* detection algorithm [12]. The first stage smooths the ECG using a three-point moving average filter:

$$Y0(n) = [X(n-1) + 2X(n) + X(n+1)]/4$$

$$1 < n < 8190.$$

The output of the moving point averaging filter is passed through a low-pass filter.

$$Y1(n) = [1/(2m+1)] \sum_{k=n-m}^{n+m} Y0(k)$$

$$m < n < 8191 - m.$$

The difference between the input and output of the low-pass filter is squared:

$$Y2(n) = (Y0(n) - Y1(n))^2 \quad m < n < 8191 - m.$$

The squared difference is filtered:

$$Y3(n) = Y2(n) \left\{ \sum_{k=n-m}^{n+m} Y2(k) \right\}^2$$

$$m < n < 8191 - m.$$

A fourth array is formed using the following formula:

$$Y4(n) = Y3(n) \quad \text{if } [(Y0(n) - Y0(n - m)) \\ [Y0(n) - Y0(n + m)] > 0 \\ Y4(n) = 0 \quad \text{otherwise.}$$

The maximum value of this array is determined and scaled to form the threshold:

$$\text{Threshold} = 0.125 \max [Y4(n)] \\ m < n < 8191 - m.$$

A *QRS* candidate occurs when a point in $Y4(n)$ exceeds the threshold:

If $Y4(n) > \text{threshold}$ then, *QRS* candidate.

Okada suggests setting m equal to three for best results; however, it was determined using the tuning procedure that larger values of m result in improved performance for several types of noise. As m increases the performance increases along with computational demands. The improvement in performance begins to fall off at values of m greater than four while the computational demands continue to increase. The value of m was set to six in order to give good performance while keeping the computational requirements at a reasonable level.

VI. RESULTS

The results from this experiment are listed in Tables I-V. Each table gives the results for all of the algorithms for all levels of a given type of noise.

A. Electromyographic Noise

The first table gives the results for the effects of electromyographic noise. This noise type has broad-band frequency characteristics which overlap the frequency spectrum of the *QRS* complex. The amplitude of the *QRS* complex is, however, considerably greater than the noise. The ability of algorithm AF2 to correctly identify all of the *QRS* complexes without incurring any false positives can be attributed to this fact. The noise is effectively eliminated in AF2 on the basis of its amplitude characteristics. The two other algorithms based on amplitude and slope do not perform nearly as well. At the maximum noise corruption level, neither AF1 or AF3 is able to locate more than 65 percent of the *QRS* complexes and each have more false positives than *QRS* complexes detected.

The failure of algorithms AF1 and AF3 to achieve the results obtained by AF2 is a consequence of the method for selecting the value of the scaling constant. The value of the scaling constant is obtained via the tuning procedure while the algorithm operates on the composite noise-corrupted data. The composite noise has both low- and high-frequency components. Changes in baseline result in the selection of a low value for the scaling constant, otherwise *QRS* complexes on elevated baseline would be clipped. The use of the composite data in the tuning procedure requires a compromise in the selection of constants

for all of the algorithms. The results for a given noise type can often be improved if the algorithm parameters are selected specifically for that noise type instead of the composite noise, as is the case in this study.

A few general comments seem appropriate at this point. Altering the algorithm parameters may reduce the number of false positives generated by a given algorithm for a given noise type. In many cases, the number of detected *QRS* complexes will also drop. If an algorithm is unable to detect all of the *QRS* complexes without generating false positives for any set of parameters, then it has a poor ability to discriminate between that noise type and the *QRS* complex. Each algorithm has a maximum potential to discriminate between noise and the *QRS*, which depends on the optimum selection of parameters. The best choice of parameters for the composite noise may not yield the best results for any other type of noise.

Algorithm AF3 does not use amplitude in the same manner as AF1 or AF2. Algorithms AF1 and AF2 make use of the large amplitude of the *R*-wave whereas AF3 only requires that the product of slope and amplitude be positive. It is not possible to reconfigure this algorithm to filter the noise on the basis of amplitude as it is with the previous two algorithms, AF1 and AF2.

Algorithms based on derivatives only have the worst performance of all. Electromyographic noise has first and second derivative characteristics that are similar to those of the *QRS* complex. Algorithm FD1 is able to detect all 37 *QRS* complexes, but it has more than five times that many false positives. Other algorithms in this class demonstrate an even poorer ability to discriminate between *QRS* and noise. FD2 is the worst, locating 32 of 37 *QRS* complexes with 417 false positives.

The digital filters have lower levels of false positives than the algorithms based on first or first and second derivatives, but they are unable to locate all of the *QRS* complexes. It is possible that the *QRS* complexes are suppressed along with the noise by the filtering algorithms.

B. Powerline Interference

The results for the 60 Hz powerline interference, listed in Table II, are considerably better than those for the EMG interference. The frequency spectrum for the powerline interference consists only of the 60 Hz fundamental and first harmonic. Five of the algorithms are able to correctly locate all of the 37 *QRS* complexes. Four of these, AF2, FD1, DF1, and DF2 are able to do so without generating any false positives. Only one algorithm gives false positives at the highest noise level, although a second did at intermediate noise levels.

Powerline interference at the 100 percent level is able to effectively mask all *QRS* complexes from algorithms AF3 and FS1. These algorithms give no false positives and do not detect any *QRS* complexes at this noise level. In some systems, such as patient monitoring, this characteristic may be advantageous since the prolonged absence of output from a detector is a clear indication of a

TABLE I
ELECTROMYOGRAPHIC (EMG)

	% QRS Detected					No. of False Positives				
	0	25	50	75	100	0	25	50	75	100
AF1	100	100	86	73	65	0	0	3	19	48
AF2	100	100	100	100	100	0	0	0	0	0
AF3	100	100	95	65	51	0	8	20	30	31
FD1	100	100	100	97	97	0	0	0	86	207
FD2	100	100	95	92	86	0	0	69	257	417
FS1	100	92	76	81	62	0	47	322	335	278
FS2	100	43	30	27	27	0	0	12	40	64
DF1	100	100	100	95	84	0	0	0	1	36
DF2	100	97	78	62	62	0	0	0	1	13

TABLE II
POWERLINE INTERFERENCE

	% QRS Detected					No. of False Positives				
	0	25	50	75	100	0	25	50	75	100
AF1	100	100	59	59	19	0	0	0	0	0
AF2	100	100	100	100	100	0	0	0	0	0
AF3	100	100	19	0	0	0	0	0	0	0
FD1	100	100	100	100	100	0	0	0	0	0
FD2	100	100	59	59	59	0	0	0	0	0
FS1	100	78	100	22	0	0	297	0	0	0
FS2	100	81	100	100	100	0	0	0	8	15
DF1	100	100	100	100	100	0	0	0	0	0
DF2	100	100	100	100	100	0	0	0	0	0

problem requiring human intervention. This may be preferable to a system which gives low numbers of false positives since this condition may be more difficult to detect. However, an algorithm which can discriminate between 60 Hz noise and QRS complexes would always be preferable if it has the other required characteristics.

C. Respiration

Baseline drift due to respiration presents a lesser challenge to all of the algorithms except those based on amplitude and first derivative. The results for this noise type are listed in Table III. All of the other algorithms give ideal performance. Low-frequency noise of this type is apparently ignored by algorithms based exclusively on derivatives or by algorithms using digital filters.

Algorithms which utilize amplitude are compromised by the change in amplitude of the QRS complexes due to large changes in baseline. Since absolute amplitude is used as a criterion for identification, QRS complexes at or near a minimum (trough) of the respiratory cycle may not have sufficient amplitude to meet the criterion. Since these algorithms operate on amplitude rather than frequency, the QRS complexes are filtered along with the noise.

D. Baseline Shift

Abrupt baseline shift is a slightly greater challenge than the baseline drift due to respiration. The results for this

noise type are listed in Table IV. Although four of the algorithms are able to locate all QRS complexes without generating any false positives, a majority of the algorithms exhibit some decrease in performance. Only two algorithms, FD1 and DF2, have any false positives. Both detect all QRS complexes correctly and have approximately 20–30 percent as many false positives as correct detections.

DF1 suffers only a very slight decrease in performance at the highest noise level by missing one QRS complex. Only FS2 has significant difficulty locating QRS complexes, missing all of them at higher levels of baseline shift. AF2 also experiences a lesser degree of difficulty. This is a consequence of the change in amplitude of several of the QRS complexes as in the case of baseline drift due to respiration. The other algorithms based on amplitude are not affected since the maximum change in amplitude is less for the abrupt baseline shift as compared to the baseline drift due to respiration.

E. Composite Noise

Composite noise was as great a challenge as electromyographic noise since only one algorithm, DF1, was able to detect all QRS complexes without any false positives. Refer to Table V for the results. Algorithms FD1 and DF2 gave reasonable results at the 75 percent noise level. Algorithms AF2, FD2, and FS1 were very sensitive

TABLE III
RESPIRATION (RESP)

	% QRS Detected					No. of False Positives				
	0	25	50	75	100	0	25	50	75	100
AF1	100	100	100	76	65	0	0	0	0	0
AF2	100	100	65	57	54	0	0	0	0	0
AF3	100	100	100	86	76	0	0	0	4	6
FD1	100	100	100	100	100	0	0	0	0	0
FD2	100	100	100	100	100	0	0	0	0	0
FS1	100	100	100	100	100	0	0	0	0	0
FS2	100	100	100	100	100	0	0	0	0	0
DF1	100	100	100	100	100	0	0	0	0	0
DF2	100	100	100	100	100	0	0	0	0	0

TABLE IV
BASELINE SHIFT

	% QRS Detected					No. of False Positives				
	0	25	50	75	100	0	25	50	75	100
AF1	100	100	100	100	100	0	0	0	0	0
AF2	100	100	100	59	59	0	0	0	0	0
AF3	100	100	100	100	100	0	0	0	0	0
FD1	100	100	100	100	100	0	0	6	12	6
FD2	100	100	100	100	100	0	0	0	0	0
FS1	100	100	100	100	100	0	0	0	0	0
FS2	100	100	3	0	0	0	0	0	0	0
DF1	100	100	100	97	97	0	0	0	0	0
DF2	100	100	100	100	100	0	0	0	9	13

TABLE V
COMPOSITE NOISE

	% QRS Detected					No. of False Positives				
	0	25	50	75	100	0	25	50	75	100
AF1	100	100	95	81	70	0	0	0	3	7
AF2	100	100	84	73	70	0	0	0	13	75
AF3	100	100	92	54	32	0	0	2	4	6
FD1	100	100	100	100	97	0	0	0	1	4
FD2	100	100	100	92	86	0	0	0	13	62
FS1	100	70	59	76	78	0	20	283	321	272
FS2	100	43	24	22	19	0	0	0	6	20
DF1	100	100	100	100	100	0	0	0	0	0
DF2	100	100	100	95	84	0	0	0	0	0

to the maximum noise level, resulting in a very high rate of false positives.

Although the individual noise types are scaled down before they are combined to form the composite noise, the results are generally worse than for the individual noise types. The combination of the various noise types has a synergistic effect decreasing the performance. Composite noise is a more realistic model of the noise problem which would be expected in a clinical setting.

F. QRS Detection Delay

Now let us briefly discuss the delay time in QRS detection. In most cases the number of sample points delay in QRS detection remained relatively constant at two to three

samples despite increases in noise level. Two exceptions should be noted. Algorithms FS1 and FS2 had the lowest detection delay for the clean ECG, 0.0 and 1.0 sample points, respectively. At low-noise levels for either EMG, powerline or composite noise, the delay increases to a range of 4 to 8 sample points. This suggests that these two algorithms have difficulty distinguishing between high frequency noise and the QRS onset. Since the delay for the other algorithms is relatively consistent, the actual onset can be approximated by subtracting a fixed delay from the candidate onset. It may be preferable to search for the peak which is more precisely defined (using techniques such as template matching) in systems which require accurate fiducial point determination.

VII. CONCLUSION

No single algorithm evaluated in this study is clearly superior for all of the types of noise considered. For many applications DF1 would be the obvious choice since it can best handle combinations of noise if the contribution from each of the individual noise types can be limited. The effectiveness of algorithm DF1 can be in part attributed to the powerline notch filter which could also be used in a preprocessing stage for any of the algorithms.

Algorithms based on amplitude and slope are most immune to EMG noise. Since this type of noise presents the greatest challenge, these algorithms have a significant advantage. These algorithms are sensitive to changes in baseline which accounts for the decrease in performance when subjected to composite noise. If changes in baseline can be corrected by high pass filtering and/or a cubic spline technique [13], these algorithms would offer the highest performance. Filtering EMG noise is more difficult due to the frequency spectrum overlap with the QRS complex, therefore algorithms which are insensitive to baseline changes but sensitive to high frequency noise have less potential than the amplitude-slope algorithm or reliable performance in a clinical setting.

The ability of the algorithms to recognize different forms of normal or abnormal QRS complexes or to ignore large peaked T-waves was not tested. Most instrumentation systems utilize more than one channel (ECG lead) and each channel presents a different waveform. The signal used in this study was obtained from a limb lead (II). No attempt was made to run the algorithms on a signal which would represent the signal obtained from other ECG leads.

The limitations described above do not seriously compromise the usefulness of these results for many applications. The performance of these algorithms was in part attributable to the tuning procedure. This procedure would not be practical in a clinical setting, but adaptive mechanisms could be developed to configure the algorithms during an initial learning phase to a patient's unique QRS complex. It is probable that multichannel systems could have even higher performance, perhaps by the incorporation of a voting scheme or signal processing methods. This study provides useful information about the noise properties of the nine algorithms. These results will prove valuable to those who use QRS algorithms similar to the ones presented in this study.

ACKNOWLEDGMENT

The authors wish to acknowledge the support of the Engineering Experiment Station at Auburn University and the North Carolina Biotechnology Center. They also wish to thank Dr. J. Buchanan of the University of North Carolina at Chapel Hill for his thoughtful comments and review of the manuscript.

REFERENCES

- [1] John G. Webster, Ed., *Medical Instrumentation—Application and Design*. Boston: Houghton Mifflin, 1978.
- [2] G. S. Furno and W. J. Tompkins, "A learning filter for reducing noise interference," *IEEE Trans. Biomed. Eng.*, vol. BME-30, pp. 234–235, 1983.
- [3] W. F. Ganong, *Review of Medical Physiology*, 11th ed. Los Altos, CA: Lange Medical, 1983.
- [4] P. M. Mahoudeux *et al.*, "Simple microprocessor-based system for on-line ECG analysis," *Med. Biol. Eng. Comput.*, vol. 19, pp. 497–500, 1981.
- [5] J. Fraden and M. R. Neuman, "QRS wave detection," *Med. Biol. Eng. Comput.*, vol. 18, pp. 125–132, 1980.
- [6] D. Gustafson *et al.*, "Automated VCG interpretation studies using signal analysis techniques," R-1044 Charles Stark Draper Lab., Cambridge, MA, 1977.
- [7] A. Menrad *et al.*, "Dual microprocessor system for cardiovascular data acquisition, processing and recording," in *Proc. 1981 IEEE Int. Conf. Industrial Elect. Contr. Instrument.*, 1981, pp. 197–205.
- [8] W. P. Holsinger *et al.*, "A QRS preprocessor based on digital differentiation," *IEEE Trans. Biomed. Eng.*, vol. BME-18, pp. 212–217, 1971.
- [9] R. A. Balda *et al.*, "The HP ECG analysis program," *Trends in Computer-Processed Electrocardiograms*, J. H. vanBemmel and J. L. Willems, Eds. North Holland, 1977, pp. 197–205.
- [10] M. L. Ahlstrom and W. J. Tompkins, "Automated high-speed analysis of holter tapes with microcomputers," *IEEE Trans. Biomed. Eng.*, vol. BME-30, pp. 651–657, Oct. 1983.
- [11] W. A. H. Engelse and C. Zeelenberg, "A single scan algorithm for QRS-detection and feature extraction," *IEEE Comput. Card.*, Long Beach: IEEE Computer Society, 1979, pp. 37–42.
- [12] M. Okada, "A digital filter for the QRS complex detection," *IEEE Trans. Biomed. Eng.*, vol. BME-26, pp. 700–703, Dec. 1979.
- [13] C. R. Meyer and H. N. Keiser, "Electrocardiogram baseline noise estimation and removal using cubic splines and state-space computation techniques," *Comput. Biomed. Res.*, vol. 10, pp. 459–470, 1977.
- [14] C. S. Weaver *et al.*, "Digital filtering with applications to electrocardiogram processing," *IEEE Trans. Audio Electroacoust.*, vol. AU-16, pp. 350–389, Sept. 1968.
- [15] H. K. Wolf, J. D. Sherwood, and J. D. Kanon, "The effect of noise on the performance of several ECG programs," *Proc. Comput. Cardiol.*, pp. 303–304, 1976.
- [16] G. J. H. Uijen, J. P. C. de Weerd, and A. J. H. Vendrik, "Accuracy of QRS detection in relation to the analysis of high-frequency components in the electrocardiogram," *Med. Biol. Eng. Comput.*, vol. 17, pp. 492–502, July, 1979.
- [17] C. N. Mead *et al.*, "Development and evaluation of a new QRS detector/delineator," *Proc. Comput. Cardiol.*, pp. 251–254, Sept. 1979.
- [18] L. Sörnmo *et al.*, "A mathematical approach to QRS detection," *Proc. Comput. Cardiol.*, pp. 205–208, 1980.
- [19] A. L. Goldberg and V. Bhargava, "Peak-to-peak amplitude of the high-frequency QRS: A simple, quantitative index of high-frequency potentials," *Comput. Biomed. Res.*, vol. 14, pp. 399–406, 1981.
- [20] L. Sörnmo *et al.*, "A method of evaluating QRS shapes features using a mathematical model for the ECG," *IEEE Trans. Biomed. Eng.*, vol. BME-28, pp. 713–717, Oct. 1981.
- [21] A. L. Goldberg and V. Bhargava, "Computerized measurement of the first derivative of the QRS complex: Theoretical and practical considerations," *Comput. Biomed. Res.*, vol. 14, pp. 464–471, 1981.
- [22] S. Blumlein *et al.*, "Detection of signal associated with noise," *Proc. Comput. Cardiol.*, pp. 339–342, 1981.
- [23] T. Fancott *et al.*, "Design considerations for noise immunity in the concordia high speed ambulatory ECG tape analysis system," *Proc. Comput. Cardiol.*, pp. 343–346, 1981.
- [24] M. Nygård and L. Sörnmo, "A QRS delineation algorithm with low sensitivity to noise and morphology changes," *Proc. Comput. Cardiol.*, pp. 347–350, 1981.
- [25] C. N. Mead *et al.*, "A frequency-domain-based QRS classification algorithm," *Proc. Comput. Cardiol.*, pp. 351–354, 1981.
- [26] F. E. M. Brekelmans and C. D. R. de Vaal, "A QRS detection scheme for multichannel ECG devices," *Proc. Comput. Cardiol.*, pp. 437–440, 1981.
- [27] R. A. A. F. van Dam, F. E. M. Brekelmans, and J. S. Duisterhout, "A high performance microprocessor-based arrhythmia monitor," *Proc. Comput. Cardiol.*, pp. 449–452, 1981.
- [28] J. L. Talmon and A. Hasman, "A new approach to QRS-detection and typification," *Proc. Comput. Cardiol.*, pp. 479–482, 1981.
- [29] P. O. Börjesson *et al.*, "Adaptive QRS detection based on maximum a posteriori estimation," *IEEE Trans. Biomed. Eng.*, vol. BME-29, pp. 341–351, 1982.

- [30] A. V. Sahakian, W. J. Tompkins, B. M. Tompkins, and J. K. Kreul, "A microprocessor-based arrhythmia monitor/recorder for the operating and recovery rooms," *Med. Instrument.*, vol. 17, pp. 131-134, Mar.-Apr. 1983.
- [31] N. V. Thakor, J. G. Webster, and W. J. Tompkins, "Optimal QRS detection," *Med. Biol. Eng. Comput.*, vol. 21, pp. 343-350, May 1983.
- [32] —, "Estimation of QRS complex power spectra for design of a QRS filter," *IEEE Trans. Biomed. Eng.*, vol. BME-31, pp. 702-706, Nov. 1984.
- [33] J. Pan and W. J. Tompkins, "A real-time QRS detection algorithm," *IEEE Trans. Biomed. Eng.*, vol. BME-32, pp. 230-236, Mar. 1985.
- [34] L. Sörnmo, O. Pahlm, and M. Nygård, "Adaptive QRS detection: A study of performance," *IEEE Trans. Biomed. Eng.*, vol. BME-32, pp. 392-401, June 1985.
- [35] M. L. Ahlstrom and W. J. Tompkins, "Digital filters for real-time ECG signal processing using microprocessors," *IEEE Trans. Biomed. Eng.*, vol. BME-32, pp. 708-713, Sept. 1985.
- [36] J. A. van Alsté and T. S. Schilder, "Removal of base-line wander and power-line interference from the ECG by an efficient FIR filter with a reduced number of taps," *IEEE Trans. Biomed. Eng.*, vol. BME-32, pp. 1052-1060, Dec. 1985.
- [37] P. S. Hamilton and W. J. Tompkins, "Quantitative investigation of QRS detection rules using the MIT/BIH arrhythmia database," *IEEE Trans. Biomed. Eng.*, vol. BME-33, pp. 1157-1165, Dec. 1986.



Manal Afify Jadallah was born in Alexandria, Egypt, on September 7, 1964. She received the B.S.E.E. degree from North Carolina State University, Raleigh, in 1987.

She is currently working for the Research and Development Department of Alcatel Network Systems and pursuing a Masters degree in electrical engineering. Her work on QRS algorithms was done while pursuing the baccalaureate degree. She is now involved in microcontroller board level design for telecommunication systems under develop-

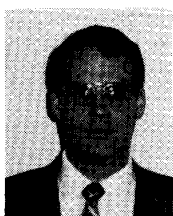
ment at Alcatel.



Stanford L. Yates was born in Cincinnati, OH, on July 28, 1962. He received the B.S.E.E. degree from North Carolina State University, Raleigh, in 1987.

Since then, he has worked for Bell Northern Research in Research Triangle Park, NC. His current interests include real-time computing, medical electronics, and digital signal processing.

Mr. Yates is a member of Phi Kappa Phi and Tau Beta Pi.



Gary M. Friesen was born in Long Beach, CA, on May 7, 1957. He received the B.E.E. degree from Auburn University, Auburn, AL, in 1980. From 1981 until 1985 he pursued graduate studies in physiology and electrical engineering at Auburn University in the areas of the pathophysiology of hypovolemic shock and medical instrumentation.

He is currently completing the requirements for the M.S.E.E. degree from Auburn University and the M.D. degree from the University of South Al-

abama, Mobile.



Thomas C. Jannett (M'80) received the B.S. degree in engineering and the M.S. degree in biomedical engineering in 1979 and 1981, respectively, from The University of Alabama, Birmingham, and the Ph.D. degree in electrical engineering from Auburn University, Auburn, in 1986.

He is Assistant Professor of Electrical Engineering and Biomedical Engineering at The University of Alabama at Birmingham. His research interests include automated drug delivery systems, medical instrumentation, and system identification.

tification.

Stephen R. Quint (S'69-M'69-M'82), photograph and biography not available at the time of publication.



H. Troy Nagle (S'66-M'70-SM'74-F'83) was born in Booneville, MS, on August 31, 1942. He received the B.S.E.E. and M.S.E.E. degrees from the University of Alabama, University, in 1964 and 1966, the Ph.D. degree from Auburn University, Auburn, AL, in electrical engineering in 1968, and the M.D. degree from the University of Miami School of Medicine, Coral Gables, FL, in 1981.

He is a Professor of Electrical and Computer Engineering at North Carolina State University, Raleigh, and Research Professor in the Biomedical Engineering Curriculum at the University of North Carolina, Chapel Hill. He is widely published in data acquisition and control systems. He is coauthor of textbooks in digital local design and sampled-data-control systems. His current areas of research are fault-tolerant systems design, design for testability, and medical instrumentation.

Dr. Nagle is a member of Phi Kappa Phi, Tau Beta Pi, Eta Kappa Nu, Sigma Xi, and Omicron Delta Kappa. He is listed in *Who's Who in America*, and is the recipient of the IEEE Centennial Medal. He was President of the Industrial Electronics Society in 1984 and 1985, Vice-President for Area Activities of the Computer Society in 1986, and a member of the IEEE Board of Directors representing the Computer Society during 1987 and 1988. He is currently the Vice President for Technical Activities of the IEEE.